applied sciences

MDPI

Article

Mechanical Sealing Method for Laboratory-Scale Hydraulic Fracturing Tests of Granite Rocks Under High-Temperature and High-Pressure Conditions

Zhang Hongwei [1,2,3,4], Chen Zhaoying [1,*], Zhou Chuanhong [2], Yang Qingshuai [2], Rui Xusheng [2] and Wang Shijun [2]

[1] State Key Laboratory of Coal and CBM Co-Mining, Jincheng 048000, China; hongwei@cumtb.edu.cn
[2] School of Energy and Mining Engineering, China University of Mining and Technology (Beijing), Beijing 100083, China; zch8535@163.com (Z.C.); bronyang@163.com (Y.Q.); rxsping@163.com (R.X.); 15502990328@139.com (W.S.)
[3] Engineering Research Center of Green and Intelligent Mining for Thick Coal Seam, Ministry of Education, Beijing 100083, China
[4] Engineering Research Center of Geothermal Resources Development Technology and Equipment, Ministry of Education, Jilin University, Changchun 130026, China
* Correspondence: chenzhaoying2008@163.com

Abstract: Deep hot dry rock (HDR) geothermal energy is a widespread and sustainable renewable energy that could be extracted for the decarbonisation of electricity generation. Measurements are essential for hydraulic fracturing in HDR monitoring, which can be used for assessing the current state and predicting the future performance of geothermal systems. However, a major challenge is that it is difficult to implement hydraulic fracturing for HDR under high-temperature and high-pressure (HTHP) conditions. Similarly, it is hard to conduct laboratory-scale hydraulic fracturing experiments under HTHP due to the sealing failure of injection pipes in boreholes. Therefore, in this paper, we proposed a novel sealing technique by using a wedge-shaped structure for sealing injection pipes under HTHP environments. By conducting numerical simulations and experimental verifications, we discovered that (1) compression stress should be applied on the seal to achieve pre-sealing. Specifically, a compression displacement of between 2 mm and 6 mm is suggested. (2) Copper material with good ductility, high-temperature bearing performance, and excellent thermal expansion is preferred for manufacturing the seal components. (3) Heating-induced thermal expansion of sealing is conducive to re-sealing rocks.

Keywords: sealing technique; hydraulic fracturing; high temperature and high pressure

Citation: Hongwei, Z.; Zhaoying, C.; Chuanhong, Z.; Qingshuai, Y.; Xusheng, R.; Shijun, W. Mechanical Sealing Method for Laboratory-Scale Hydraulic Fracturing Tests of Granite Rocks Under High-Temperature and High-Pressure Conditions. *Appl. Sci.* **2024**, *14*, 10255. https://doi.org/10.3390/app142210255

Academic Editor: Tiago Miranda

Received: 15 July 2024
Revised: 10 October 2024
Accepted: 29 October 2024
Published: 7 November 2024

1. Introduction

Geothermal energy is heat that is generated within the Earth. It is a clean, renewable resource that can be harnessed for heat and electricity production. Hot dry rock (HDR) is a kind of high-quality, widespread, and abundant geothermal resource [1]. It refers to the naturally occurring hot rocks deep within the Earth's crust that are not associated with magma or volcanic activity. These rocks are typically found at depths of 3 to 10 km, with temperatures ranging from 150 to 650 °C. The potential of HDR geothermal energy is vast, as it is estimated to be many times greater than the energy that can be harnessed from traditional hydrothermal resources. Formations consisting primarily of granites that have high temperatures but very low permeability and lack stored fluid are candidates for HDR development. Therefore, to explore the heat in the HDR reservoir, stimulation techniques are commonly applied to enhance the permeability of the target formations [2]; otherwise, the HDR is too impermeable to allow for sufficient fluid circulation.

Hydraulic fracturing has been widely used in exploration to increase the permeability of deep geothermal reservoirs (Figure 1a). The effectiveness of hydraulic fracturing is contingent upon the performance of frac plugs. Current fracturing plugs always use a

rubber material to achieve sealing, but they are not well sealed under the evaluated temperature due to heating-induced rubber crushing or rupturing. Meanwhile, laboratory-scale hydraulic fracturing tests of magmatic rocks under high-temperature and high-pressure (HTHP) conditions are normally conducted to understand the hydraulic fracturing characteristics of rocks [3,4]. However, due to the poor high-temperature (above 200 °C) tolerance of sealing materials, the hydraulic fracturing tests under HTHP are also rarely achieved [5], and fluid leak-offs or seal failures between casing pipes and boreholes always occur. Therefore, developing a novel high-temperature sealing technique is of great significance for facilitating hydraulic fracturing tests under HTHP conditions.

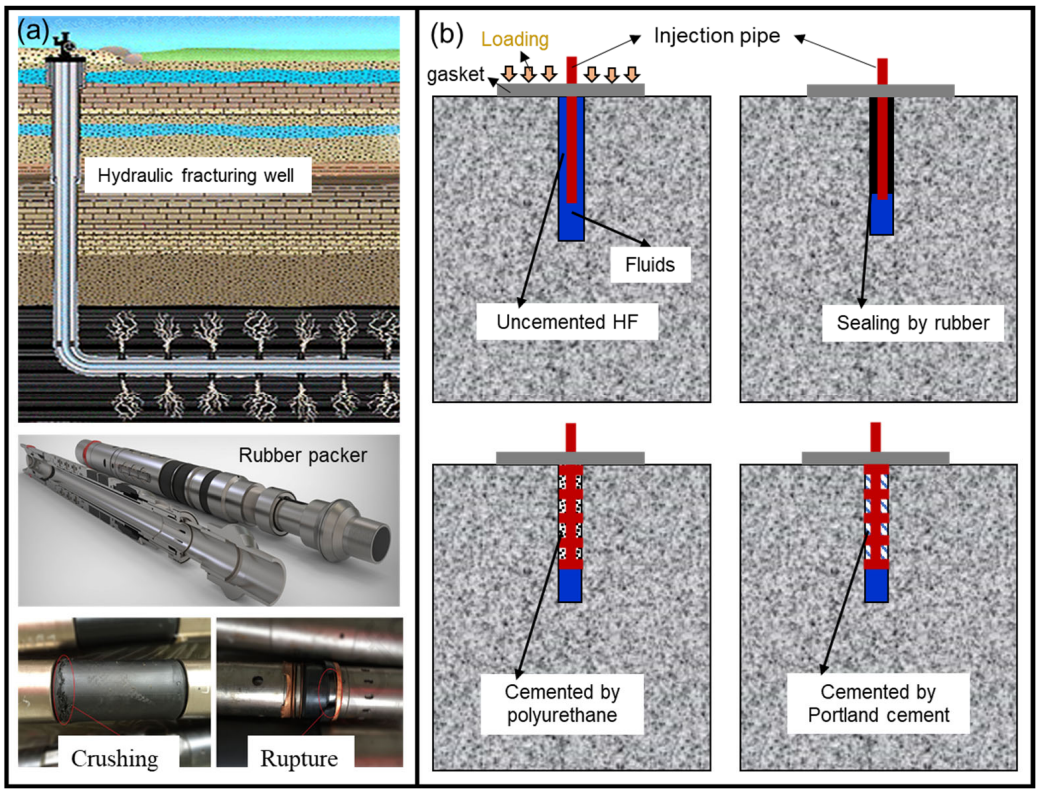

Figure 1. Packers and sealing methods for the hydraulic fracturing test. (**a**) In situ hydraulic fracturing and failure modes of a rubber packer; (**b**) open-hole hydraulic fracturing with uncemented pipe, rubber sealing, and other chemical sealant sealing methods.

To date, most high-temperature hydraulic fracturing tests have been conducted at 200 °C (Table 1). Among these tests, small samples (e.g., φ50 × 100 mm) and the open-hole fracturing method have been generally adopted. The open-hole hydraulic fracturing method can avoid leak-offs because it employs a compress-sealed gasket on the end surface of samples. The disadvantage of a small sample is that it is difficult to study the propagation of fractures and re-fracturing mechanisms of rocks. Sealants, such as cement mortar, rubber, polyurethane, and epoxy, are also utilized for large rocks [6]. However, these sealants exhibit a propensity for softening and are susceptible to thermal cracking when subjected to elevated temperatures, which can compromise their sealing efficacy and potentially lead to the degradation of hydraulic fracturing performance over time. As shown in Figure 1, currently used sealing systems for geothermal wells, based exclusively on Portland cement systems, are not designed to withstand extreme temperatures (above 200 °C) due to various disadvantages such as heating-induced cracking and strength deterioration [7,8]. Similarly, at high temperatures (>150 °C), polymers would be thermally degraded [4]. Rubber is typically adopted due to its nonlinear viscoelastic properties [5]. However, the sealing-bearing performance of the rubber is greatly weakened in the range of 130 °C~150 °C [9], leading to it being seriously crushed or ruptured. Packers used in hydraulic fracturing

plug products are expected to be kept sealed at downhole temperatures ranging from 50 to 180 °C. Recently, efforts have been made to study the sealing properties of packer rubber. Wang et al. [10] investigated the influence of friction forces on elastomer packer sealing performance. Lan et al. [11] indicated that seals made of Tetrafluoroethylene propylene have better sealing performances than hydrogenated acrylonitrile butadiene rubber in HTHP environments. Zheng et al. [5] measured the temperature and elastomer stress relaxation effects on the rubber packer and found that an increase in temperature led to a decrease in both average contact stress and maximum contact stress. Polonsky and Tyurin [12] developed a new structure design for packers after discussing several designs aimed at enhancing sealing reliability and considering the packers' working conditions. Zeng et al. [13] conducted tests on AFLAS rubber using an HTHP autoclave in harsh environments (60 MPa, 175 °C, test period 7 days, and different corrosive gases) and analysed the changes in properties.

Table 1. Hydraulic fracturing tests under high temperatures using various sealing methods.

NO.	Temperature Range/°C	Rock Dimension/mm	Sealing Methods	Sample Types	Applied Stress/MPa	Ref.
1	20–200	300 × 300 × 300	Pre-located during sample preparation	Concrete	6~10	[14]
2	20–300	φ22.5 × 45	Open hole	Granite	0–60	[15]
3	20–120	300 × 300 × 300	Open hole	Granite	10–30	[3]
4	20–150	φ50 × 100	Open hole	Granite	5–10	[16]
5	20–200	300 × 300 × 300	Steel casing grouted by sealant	Granite	40	[17]
6	20–50	300 × 300 × 300	Steel casing grouted by epoxy	Granite	4.1–12.5	[18]
7	20–200	100 × 100 × 100	Chemical Sealant	Granite	5–10	[19]

Therefore, traditional sealing materials and techniques are not always applicable for hydraulic fracturing tests under HTHP conditions. In this paper, a novel mechanical sealing method is proposed. Firstly, the structure of the sealing material and its assembly method is introduced. Afterwards, the physical and mechanical properties of the sealing material are measured. Finally, hydraulic fracturing tests using the proposed sealing materials under HTHP conditions are performed.

2. Sealing Method

The proposed wedge-shaped metal buckle can function well when subjected to high temperature and high pressure (Figure 2a). This sealing structure consists of caps and pedestals. The cap and pedestal can be well paired to form a complete set of seals. Two types of sealing assembly methods are proposed in this paper: single-seal and multi-seal types. Both sealing types require the placement of a central fracturing pipe for water injection. The outer diameter of the central fracturing pipe should be smaller than the inner diameter of the borehole to facilitate the placement of sealing structures. Therefore, there is a certain gap between the central fracturing pipe and the borehole. For the single-seal type, a pedestal and a cap are sequentially placed inside the central fracturing pipe, forming a wedge-shaped structure. The cap is tightened by a metal fixing rod, providing a certain amount of pre-tightening force to achieve a tight fit between the pedestal and the cap. This single-seal type is relatively simple, but the disadvantage is that it is prone to sealing failure of leaking water after the rock is first hydraulically fractured, affecting further expansion of the fracture. For the multi-seal type, a certain length of metal segmented pipe is required between each sealing structure to achieve partial or full-length sealing. Finally, a metal fixing rod is used above the top cap to provide pre-tightening force for the sealing elements. Therefore, the central fracturing pipe, sealing structure, and the rock surrounding the borehole form a unified sealing entity. The liquid enters through the central fracturing pipe to the bottom and accumulates hydraulic pressure energy at the bottom, facilitating the hydraulic fracturing process.

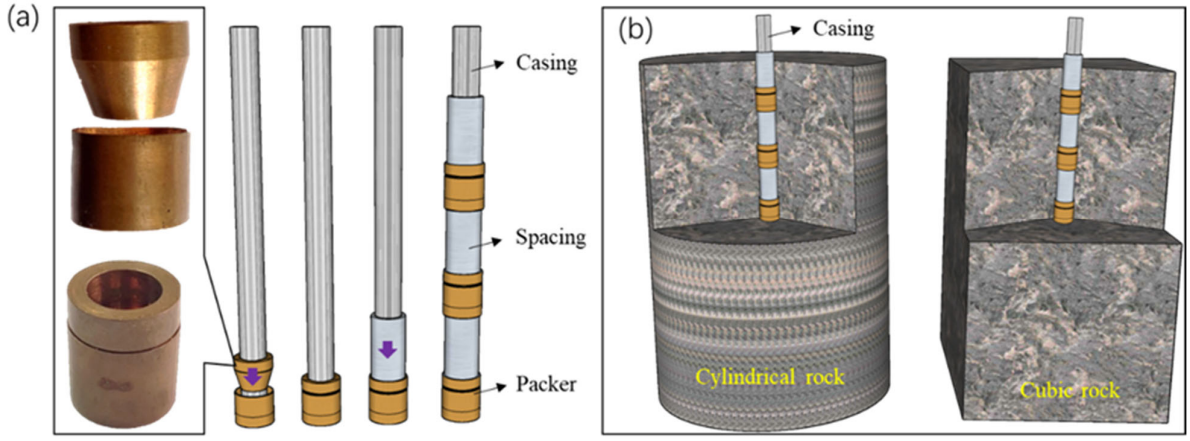

Figure 2. Sealing structures and sealed rocks. (**a**) Sealing structure and processes; (**b**) sealing in rocks.

The sealing structure could be series-connected (i.e., multi-seal type) to perform hydraulic fracturing tests of large rock samples under HTHP, such as φ200 × 400 mm, 300 × 300 × 300 mm^3, and 1000 × 1000 × 1000 mm^3, which will help to uncover the multiple hydraulic fracturing mechanisms (Figure 2b). In this study, the length of the steel ring is determined as 30 mm for granite samples with a dimension of φ200 × 400 mm. The 30 mm length refers specifically to the experimental dimensions discussed in this paper. For other specimen sizes, the dimension can be appropriately scaled up or down. The main reason for using a 30 mm spacer is to conserve sealing material. Additionally, based on the extensive experiments we have conducted, a 30 mm spacer was found to be suitable. Specifically, the easily available copper is employed to manufacture this sealing material due to its excellent ductility, large thermal expansion coefficients, and cost-effectiveness.

In the process of hydraulic fracturing, conventional sealing materials and technologies become inapplicable under HTHP conditions. For conventional packers, high temperature, high loading pressure, and high injection pressure all pose adverse risks to sealing, with high temperature being the most challenging to overcome. Therefore, the design of HTHP packers necessitates the transformation of these adverse conditions into favourable ones through alterations in sealing structures and materials. This paper develops an HTHP packer/seal using a wedge-shaped metal-interlocking structure. Regarding the sealing materials, metals with good ductility, such as copper, are selected for fabrication. This material can fill the irregularities on the surfaces of drilled holes or fracturing pipes. This material possesses excellent thermal conductivity, which can prevent uneven heating of the drilled holes caused by excessive thermal resistance of the seals. In addition, the material exhibits high-temperature sealing properties and thermal expansion characteristics, enabling close contact with the heat-emitting body, and thermal expansion can enhance sealing effectiveness.

3. Mechanical Sealing and Thermal Expansion Sealing Mechanism

3.1. Mechanical Sealing Performance

(1) Compaction response

The proposed sealing should be pre-achieved by compressing the sealing groups. To study its compressive sealing performance, the compressive loading response and deformation of sealings were directly tested using an electronic servo control testing machine (model MTS E45 (MTS Systems Corporation, Eden Prairie, MN, USA)) with a compressive displacement rate of 0.2 mm/min (Figure 3a). Two sealing samples (coated with lubricant and without lubricant) were tested to compare the friction effect of interlock surfaces of sealing components.

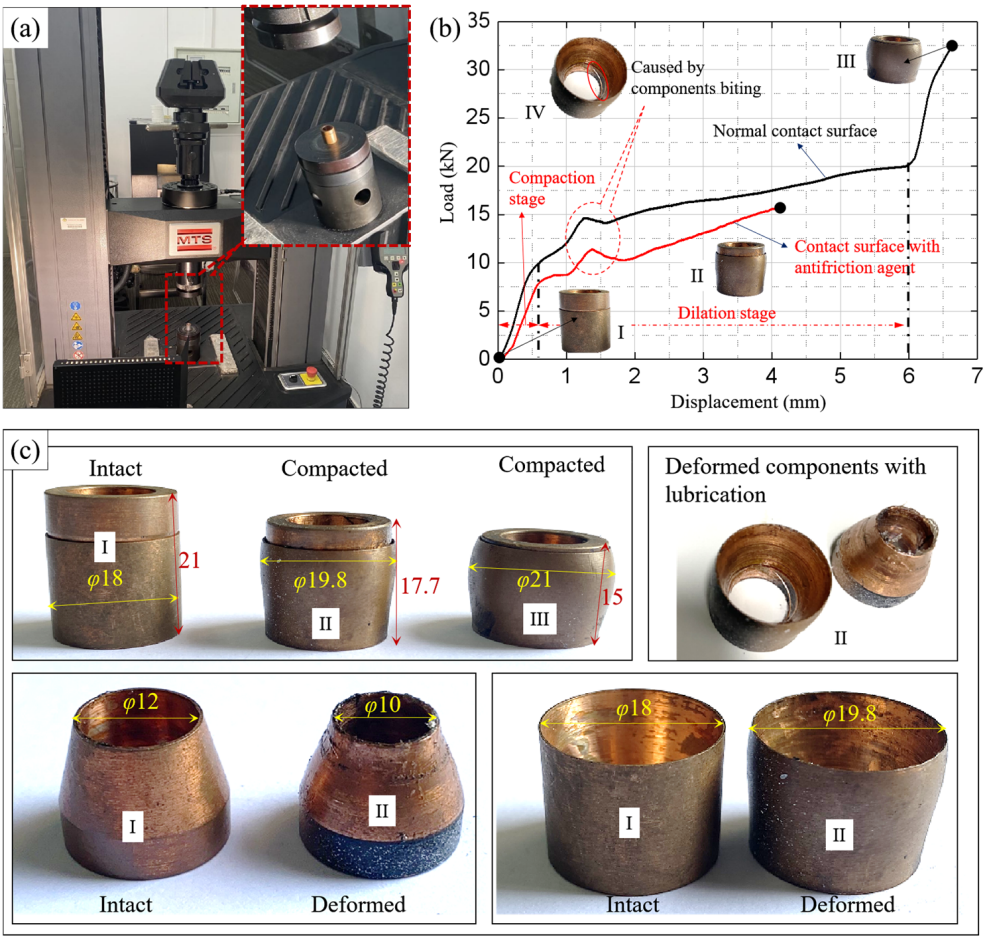

Figure 3. Test setups and materials. (**a**) Test setups; (**b**) load versus displacement curves of copper sealings; (**c**) deformation of sealing components. I: Intact; II: Compacted with a small loading; III: Compacted with a higher loading.

The compression loading response of the seal shows an overall upward trend with increasing compressive displacement (Figure 3b). Generally, three stages can be determined. First, the compression load increases sharply with displacement from 0 to 0.6 mm due to the initial contact friction during sealing-surface interlocking. As the compressive displacement increases, the compression load grows steadily, despite the loading fluctuation caused by the interlocking or biting of sealing edges. The steady increase in the loading stage ceases when the compression displacement reaches about 6 mm. Therefore, the compression displacement should be maintained at 2~6 mm during sealing. Finally, as the upper part of the seal is fully nested into the lower part, the compression load–displacement curve rises sharply due to the load-bearing capacity of the sealing components as a whole. Sealing will fail if the sealing processes are not achieved before the third compressive stage, and the dimensions of the borehole and sealings should be carefully redesigned. For seals with lubricant, the loading–displacement curve is lower than that of seals without surface treatment.

(2) Deformation of copper sealing

The deformations of sealings are shown in Figures 3 and 4. The initial dimensions of the coated sealing were $\varphi 18 \times 21$ mm. After the sample was compressed to 17.7 mm (a compression ratio of 15.7%), the sample was laterally expanded by 1.8 mm. With a completely nested displacement of 15 mm (a compression ratio of 28.6%), a lateral expansion of 3.0 mm was achieved. Therefore, the gap between the borehole and the outer surface of the seals should be smaller than 3.0 mm and a gap of about 1.8 mm is suggested.

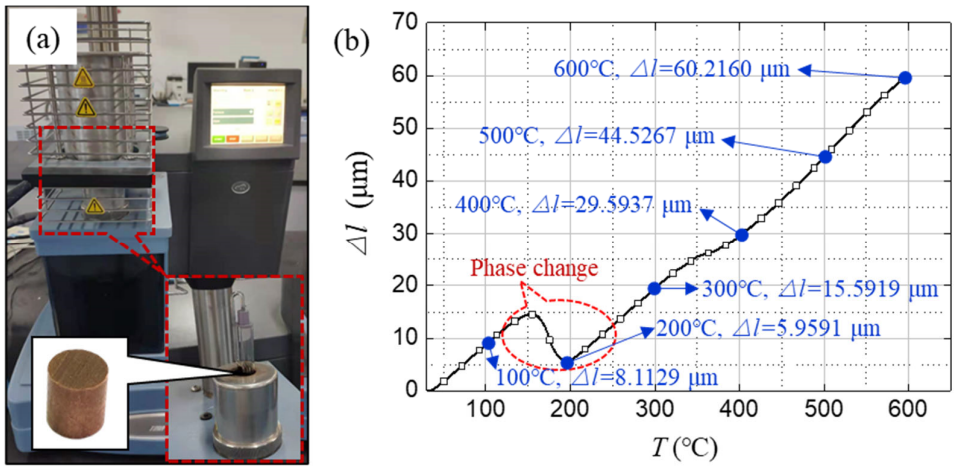

Figure 4. Thermomechanical analysis. (**a**) TMA Q400 (TA Instruments, New Castle, DE, USA) thermomechanical analysis system; (**b**) Thermal–elongation curve.

The injection pipe is located in the borehole and is locked by the inner hole surface of the seal. When the seal was compressed to 17.7 mm, the inner diameter of the upper seal component was reduced from 12 mm to 10 mm (Figure 3c). Therefore, the gap between the injection pipe and the inner surface of the seals should be less than 2.0 mm; specifically, after the installation of the injection pipe, the internal deformation of the seal is limited. Due to the thermal expansion of the injection pipe, sealings and rocks would be further sealed.

3.2. Thermal Expansion Sealing Mechanisms

The TMA Q400 thermomechanical analysis machine with a test accuracy of 10–4 μm was employed to measure the linear thermal expansion coefficient (TEC, α) of the sealing material (Figure 4a). A copper sample with a dimensions of φ8 × 9 mm was installed into a chamber to detect the continuous elongation of the sample under variable temperatures ranging from 25 °C to 600 °C. The thermal-induced elongation (Δ*l*) evolution curve is demonstrated (Figure 4b).

The copper sample's elongation generally increases with increasing temperature. The elongation decreased from 175 to 200 °C due to crystal structure transformation (Figure 4b). After 200 °C, the elongation showed an excellent thermal expansion effect; specifically, the sample was stretched by 5.9591, 15.5919, 29.5937, 44.5267, and 60.2160 μm at 200, 300, 400, 500, and 600 °C, respectively. The average TEC of the copper sample tested is 11.6654 μm/(m·°C). For the adopted isotropic sealing material in our study (φ18 × 21 mm), the lateral and axial elongations increased by 0.084 mm and 0.0980 mm at 400 °C, respectively; therefore, heating-induced expansion of sealing is conducive to re-sealing after the mechanical sealing scenario, which is a positive effect during hydraulic fracturing tests.

4. Experimental Materials and Method of Sealing Rocks Under HTHP Conditions

The Luhui granite samples (φ200 × 400 mm) were employed to conduct hydraulic fracturing tests under HTHP conditions (Figure 5). A borehole (φ18 mm × 250 mm) was drilled to install the proposed seals and injection pipes. The prepared sample was then installed into the HTHP vessel and both constant axial and confining stresses were applied at 25 MPa. Afterwards, the loaded sample was heated at a rate of 5 °C/h to the target temperatures (i.e., 100 °C, 200 °C, 300 °C, and 400 °C). After maintaining the target temperatures for over 2 h, water injection was performed. Figure 5 illustrates both the photographic images of the XPS-20 MN testing apparatus (Xuzhou Press Systems Co. Ltd., Jiangsu, China) and a detailed schematic representation of the sample setup within the HTHP vessel [20,21].

Figure 5. Test system. (**a**) The XPS-20 MN test machine; (**b**) HTHP vessel; (**c**) installation of rock in the HTHP vessel; (**d**) rock sample with casing; (**e**) surface of the granite sample after testing; (**f**) exposed picture of packers after testing.

5. Results and Discussion

Multiple hydraulic stimulation procedures were usually applied to create permeable fluid flow pathways through the hot dry rock in geothermal systems. During the hydraulic fracturing of rocks, fracturing fluid is pumped into the wellbore to increase the pressure at the bottom of the well. When this pressure is exceeded, the rock is broken and fractures are generated. When fluid injection is continued, the newly created fractures, called hydraulic or artificial fractures, grow in formation. The idealized pressure and flow rate curves are shown in Figure 6 [18]. In this figure, parameter P is the injection well pressure, Q is the fluid injection rate, t is the time, P_0 is the reservoir pore pressure, P_b is the initial fracture breakdown pressure, Ps is the fracture shut-in pressure or fracture closure pressure, and Pr is the fracture reopening pressure.

As mentioned above, fluid is pumped into the borehole to increase the pressure at the bottom during the stimulation. Fractures are generated when injection pressure exceeds the breakdown pressure. With continuous injection of fluid, fractures can be propagated and the pre-fracturing phenomenon can be revealed. According to our test results, the initial fracture breakdown pressure P_b at room temperature, 100 °C, and 200 °C were 50.6 MPa, 47.7 MPa, and 43.2 MPa, respectively. With the increase in temperature, the initial hydraulic fracturing pressure P_b dropped to 24.6 MPa at 300 °C and 15.3 MPa at 400 °C, which were

decreases of 48% and 68%, respectively, compared to that at 100 °C. Similarly, Kumari et al. [15] studied the effect of temperature on hydraulic fracturing of granite samples (φ50 × 100 mm) from room temperature to 300 °C. They found that the initial hydraulic fracturing pressure decreased linearly with increasing temperature.

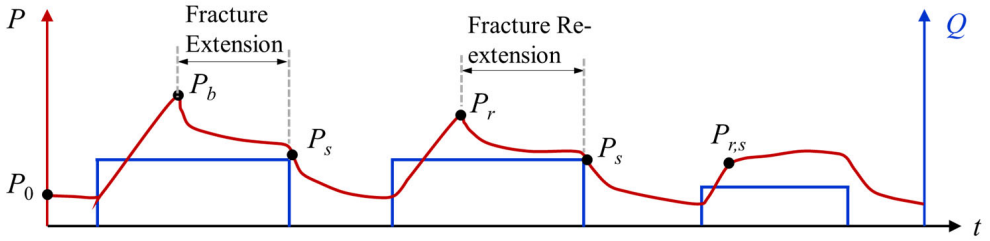

Figure 6. Idealized hydraulic fracture stimulation with three injection stages into one well.

5.1. Results of Hydraulic Fracturing of Granite Samples at Room Temperature

Figure 7 illustrates the hydraulic pressure versus time curve during the hydraulic fracturing of a granite specimen at room temperature. The specimen exhibits a high frequency of fracturing events, with seven fracturing events found. The initial fracture breakdown pressure, P_b (at 50.6 MPa), which is also the maximum fracturing pressure, occurs during the first fracturing event. The second fracturing pressure (i.e., the fracture reopening pressure, *Pr*) is the lowest of the seven fracturing events, at 37.7 MPa. The other fracture reopening pressures increase slightly with increasing fracturing events.

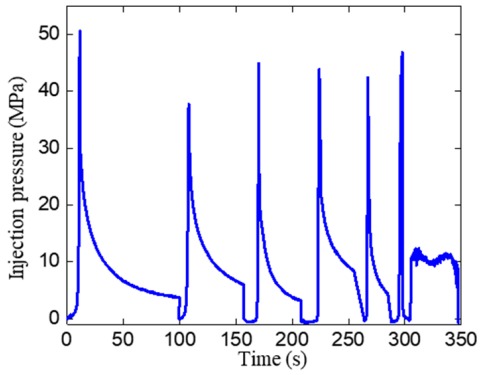

Figure 7. Injection pressure versus time curve of granite samples at room temperature.

Figure 8 presents several photos of the hydraulic fractured granite at room temperature. The dyed areas delineate the infiltration extent of the fracturing fluid during the injection process; that is to say, the fracturing fluid reached the dyed areas. The undyed areas of the fracture surface represent the areas of stress-induced failures. Visually, the fracture surface is oriented axially, with the primary fracture dividing the specimen into two halves, indicating that the propagation of the fracture spans the entire cross-sectional area. Due to the coupled effect of confining pressure and fluid pressure, the localized stress further induces the specimen into several smaller mass segments.

Figure 8. The final photos of hydraulic fractured rocks at room temperature.

5.2. Results of Hydraulic Fracturing of Granite Samples Under High Temperatures

The injection pressure versus time curve of granite samples at 100 °C is shown in Figure 9. It can be seen that, at 100 °C, complete fracturing of the specimen can be achieved with only three fracturing events, which is fewer than at room temperature. The primary reason for this is that during hydraulic fracturing at room temperature, the absence of liquid phase changes or thermal shock results in a limited depth of development of new fractures with each fracturing event. However, the rock's brittleness at room temperature is relatively higher than at high temperatures, leading to a faster fracturing rate at room temperature. At 100 °C, the first fracturing characteristic is not significantly different from that at room temperature, with an initial fracture breakdown pressure reduced by 2.9 MPa (i.e., P_b = 47.7 MPa). After the first fracturing event, the curve is steep, with a distinct closure curve. During the second water injection fracturing, the curve shows a significant change. The increase in water pressure before approaching the peak value is not linear and exhibits some fluctuations. This is distinctly different from the situation at room temperature, indicating that a small number of fractures begin to develop before the peak. After the second fracturing event, the water pressure fluctuates significantly and lasts for a longer duration. Since the sudden drop in pressure does not meet the pump shut-off conditions, the system continues to inject water into the specimen, causing the water pressure curve to decrease with fluctuations. Therefore, at 100 °C, only three water injections are needed to cause the entire specimen to fracture.

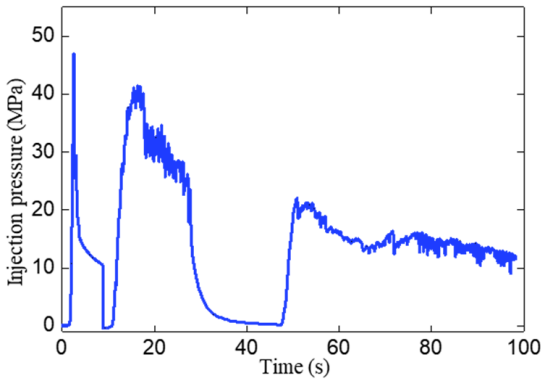

Figure 9. Injection pressure versus time curve of granite samples at 100 °C.

Figure 10 shows the injection pressure versus time curves of granite samples at 200 °C, 300 °C, and 400 °C. In comparison with Figures 7 and 9, it can be observed that from room temperature up to 200 °C, the initial fracture breakdown pressure, P_b, decreases with the increase in temperature, but the reduction is not very significant, approximately 4 MPa. Beyond 200 °C, the initial fracture breakdown pressure, P_b, experiences a sudden change as the temperature increases. The initial fracture breakdown pressure, P_b, at 300 °C and 400 °C are 24.6 MPa and 15.3 MPa. The greatest reduction in the initial fracture breakdown

pressure occurs between 200 °C and 300 °C, indicating that within this temperature range, the primary controlling condition for fracture initiation shifts towards high temperature.

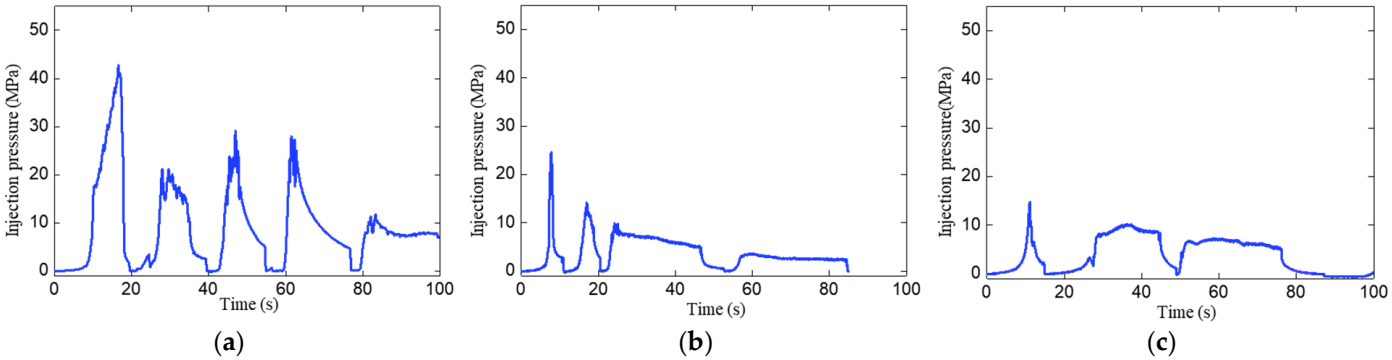

Figure 10. Injection pressure versus time curves of granite samples under different high temperatures: (**a**) 200 °C, (**b**) 300 °C, and (**c**) 400 °C.

5.3. Hydraulic Fracture Shapes and Sealings Effect Verification

Figure 11 displays the ultimate fracture morphology of the specimens after failure at various high temperatures. In contrast to the room temperature condition, where a single primary fracture divides the specimen into two major segments, at 100 °C, the specimen exhibits two pairs of symmetrical primary fractures, dividing the granite rock into four parts. At 200 °C, there is a pair of symmetrical primary fractures that split the specimen into two pieces without any branching. At 300 °C and 400 °C, the fracture patterns are highly analogous, with the specimens fracturing axially, resulting in two segments of identical size. However, unlike other temperature points, at these two temperature points (300 °C and 400 °C), one-half of the specimen in the middle presents a transverse fracture surface. These transverse fracture surfaces are not dyed, suggesting that the fracturing fluid did not penetrate the transverse fracture surface. It is postulated that the emergence of this phenomenon is due to the transverse fractures likely developing from the outside inward. During the injection of water into the specimen, the axial primary fractures open, leading to horizontal displacement of the specimen. The constraints at both ends by the press heads cause the specimen to bulge and bend outward from the middle, resulting in a breakage from the outside inward. From the experimental appearance, it is also observable that at 400 °C, the rock fracture surface is less neat, with the presence of some plastic blocks and the peeling off of some small particles. This is attributed to the transition from brittleness to plasticity in the rock at high temperatures. In general, from the perspective of sealing performance, the upper and lower inner ends of the hydraulic fractures and boreholes were not coloured, indicating that the samples were well sealed by the series-connected sealing structure.

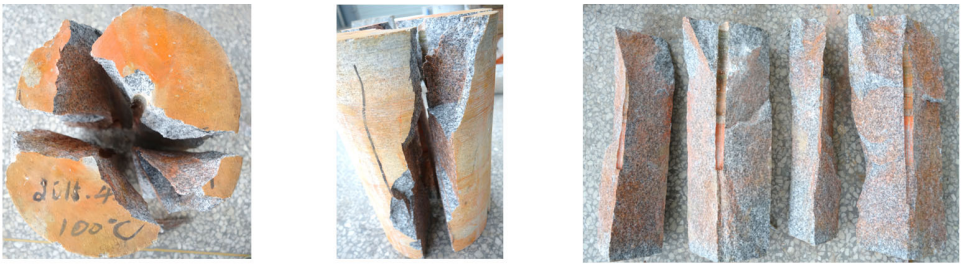

(**a**)

Figure 11. *Cont.*

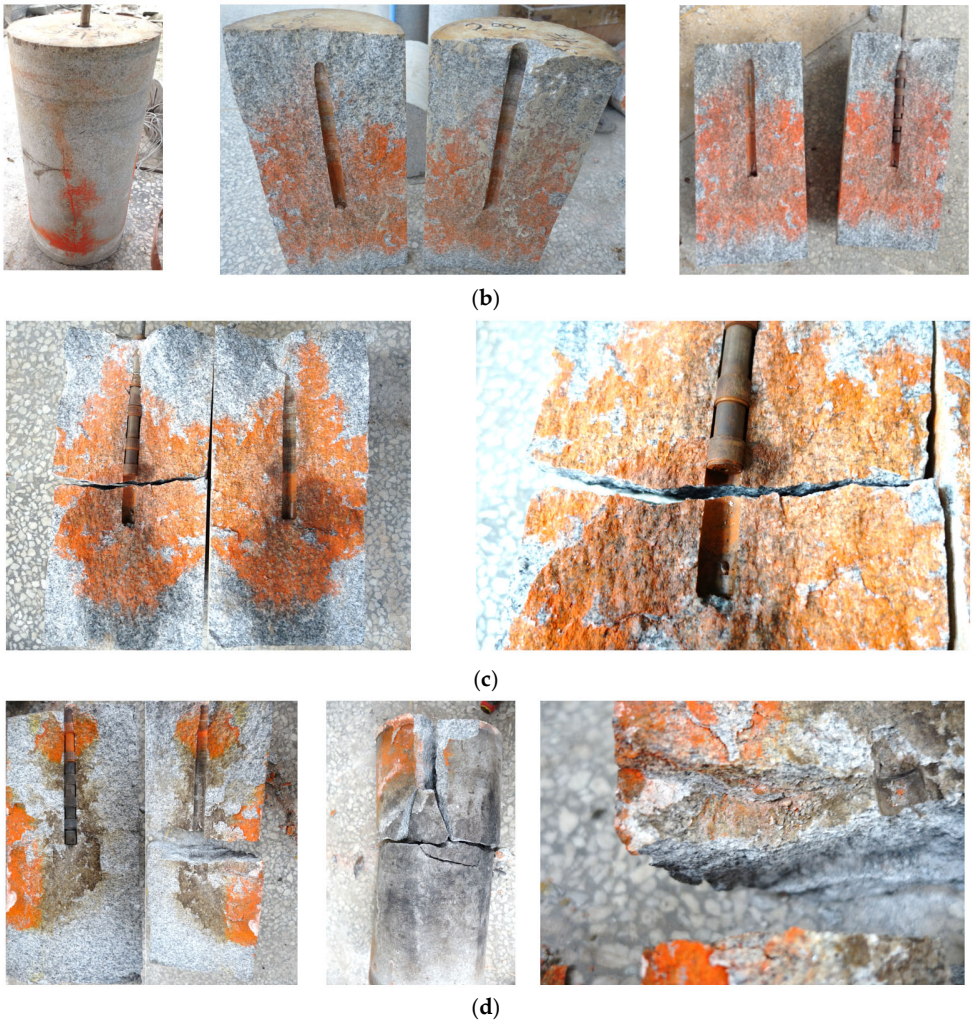

Figure 11. Hydraulic fractured granite rocks under high-temperature and high-pressure conditions. (**a**) Hydraulic fractured rocks at 100 °C; (**b**) hydraulic fractured rocks at 200 °C; (**c**) hydraulic fractured rocks at 300 °C; (**d**) Hydraulic fractured rocks at 400 °C.

5.4. Potential Applications of the Sealing Technique

As the global demand for energy continues to grow, the depth of resource acquisition is also increasing, especially in the extraction of non-renewable resources such as oil, natural gas, and oil shale. These resources are often located deep underground, where the HTHP environment poses great difficulties for mining. Hydraulic fracturing technology, as a method for increasing reservoir permeability and enhancing the capacity of production, plays an important role in the extraction of deep resources. Additionally, climate change is a global issue and clean energy must be developed to replace traditional fossil energy to reduce CO_2 emissions. HDR geothermal energy is an emerging geothermal energy source with huge energy and is also a substitute for fossil energy used for heating and generating electricity. In HDR reservoirs, the temperature of the rock is generally between 150 °C and 650 °C, and this kind of rock is buried 3–10 km underground. HDRs possess limited fractures or pore spaces and hence have no or little water, or no unified rock porousness. To harvest this geothermal heat, dry rocks are fractured by circulating cold liquid water and hydraulic pressure down one well to harvest the heat from these fractured dry rocks, and heated water is extracted from an additional geothermal well in a locked system. Therefore, whether it is the efficient extraction of deep fossil fuels or the development of renewable new energy from deep HDRs, hydraulic fracturing technology is required. However, facing HTHP environments deep underground, conventional hydraulic fracturing techniques

often fail to work, necessitating the development of new sealing equipment to adapt to such conditions.

Currently, hydraulic fracturing under HTHP conditions cannot be conducted smoothly on site. Many studies are focused on developing HTHP hydraulic fracturing isolation devices in the laboratory to achieve field-scale promotion and application. In laboratory hydraulic fracturing experiments, commonly used materials such as cement or rubber easily fail at high temperatures. Therefore, the development of a sealing technology that can remain stable in HTHP environments is particularly important. This technology can effectively solve the failure problems in high-temperature environments and is significant for both laboratory research and actual mining.

6. Conclusions

A wedge-shaped copper sealing was proposed to seal rock boreholes in laboratory-scale hydraulic fracturing tests of rocks under HTHP conditions. The sealing efficiency was verified by conducting the hydraulic fracturing tests at high temperatures ranging from 100 °C to 400 °C. Several conclusions were drawn:

(1) Before hydraulic fracturing tests, sealings in samples should be pre-tightened. A compression displacement of between 2 mm and 6 mm is suggested. The installation gap between the injection pipe and the inner surface of the seals should be less than 2.0 mm.
(2) Copper is preferred for manufacturing the seal components. The tested average TEC of copper is 11.6654 μm/(m·°C). For our sealings ($\varphi 18 \times 21$ mm), the lateral and axial elongations increased by 0.126 mm and 0.147 mm at 600 °C, respectively.
(3) The pre-tightened sealing is the controller for sealing. Heating-induced expansion of sealing is conducive to re-sealing after the mechanical sealing scenario, which is a positive effect during hydraulic fracturing tests.

Author Contributions: Z.H., C.Z., Z.H., and Z.C. analysed the data; Z.H., Z.C., Y.Q., W.S., and R.X. wrote the manuscript. All authors contributed to the final manuscript. All authors have read and agreed to the published version of the manuscript.

Funding: This research was funded by the Beijing Natural Science Foundation (no. 3232026); the National Natural Science Foundation of China (no. 52204162); the Open Research Fund Program of State Key Laboratory of Coal and CBM Co-Mining (no. 2022KF09); the Engineering Research Center of Geothermal Resources Development Technology and Equipment, Ministry of Education, Jilin University (no. 23011); and the Fundamental Research Funds for the Central Universities (No. 2023YQTD02).

Institutional Review Board Statement: Not applicable.

Informed Consent Statement: Not applicable.

Data Availability Statement: Data are contained within the article.

Acknowledgments: The authors are grateful to Ma Zhaoyang for his good suggestions during the development process.

Conflicts of Interest: The authors declare no conflict of interest.

References

1. Brown, D.W.; Duchane, D.V.; Heiken, G.; Hriscu, V.T. *Mining the Earth's Heat: Hot Dry Rock Geothermal Energy*; Springer: Berlin/Heidelberg, Germany, 2012.
2. Olasolo, P.; Juárez, M.; Morales, M.; Liarte, I. Enhanced geothermal systems (EGS): A review. *Renew. Sustain. Energy Rev.* **2016**, *56*, 133–144. [CrossRef]
3. Xing, Y.; Zhang, G.; Luo, T.; Jiang, Y.; Ning, S. Hydraulic fracturing in high-temperature granite characterized by acoustic emission. *J. Pet. Sci. Eng. Fail. Anal.* **2019**, *178*, 475–484. [CrossRef]
4. Almubarak, T.; Li, L.; Ng, J.H.; Nasr-El-Din, H.; AlKhaldi, M. New insights into hydraulic fracturing fluids used for high-temperature wells. *Pet. Geosci.* **2021**, *7*, 70–79. [CrossRef]

5. Zheng, C.; Zheng, X.; Qin, J.; Liu, P.; Aibaibu, A.; Liu, Y. Nonlinear finite element analysis on the sealing performance of rubber packer for hydraulic fracturing. *J. Nat. Gas Sci. Eng.* **2021**, *85*, 103711. [CrossRef]
6. Zhai, C.; Hao, Z.; Lin, B. Research on a New Composite Sealing Material of Gas Drainage Borehole and Its Sealing Performance. *Procedia Eng.* **2011**, *26*, 1406–1416. [CrossRef]
7. Kruszewski, M.; Glissner, M.; Hahn, S.; Wittig, V. Alkali-activated aluminosilicate sealing system for deep high-temperature well applications. *Geothermics* **2021**, *89*, 101935. [CrossRef]
8. Dong, K.; Ni, G.; Nie, B.; Xu, Y.; Wang, G.; Sun, L.; Liu, Y. Effect of polyvinyl alcohol/aluminum microcapsule expansion agent on porosity and strength of cement-based drilling sealing material. *Energy* **2021**, *224*, 119966. [CrossRef]
9. Dong, L.; Li, K.; Zhu, X.; Li, Z.; Zhang, D.; Pan, Y.; Chen, X. Study on high temperature sealing behavior of packer rubber tube based on thermal aging experiments. *Eng. Fail. Anal.* **2020**, *108*, 104321. [CrossRef]
10. Wang, P.; Chen, M.; Jenkinson, J.; Song, Y.; Sun, L. Interfacial friction effects on sealing performances of elastomer packer. *Pet. Sci.* **2024**, *21*, 2037–2047. [CrossRef]
11. Lan, W.; Wang, H.; Zhang, X.; Chen, S. Sealing properties and structure optimization of packer rubber under high pressure and high temperature. *Pet. Sci.* **2019**, *16*, 632–644. [CrossRef]
12. Polonsky, V.L.; Tyurin, A.P. Design of Packers for Sealing of the Inter-Tube Space in Equipment used for Recovery of Oil and Gas. *Chem. Pet. Eng.* **2015**, *51*, 37–40. [CrossRef]
13. Zeng, D.; Yang, X.; Zhu, D.; Zhang, Z.; Cao, D.; Chong, X.; Shi, T. Corrosion Property Testing of AFLAS Rubber under The Simulation modes of High Acid Gas Wells. *Energy Procedia* **2012**, *16*, 822–827. [CrossRef]
14. Guo, L.; Wang, Z.; Zhang, Y.; Wang, Z.; Jiang, H. Experimental and Numerical Evaluation of Hydraulic Fracturing under High Temperature and Embedded Fractures in Large Concrete Samples. *Water* **2020**, *12*, 3171. [CrossRef]
15. Kumari, W.G.P.; Ranjith, P.G.; Perera, M.S.A.; Li, X.; Li, L.H.; Chen, B.K.; AvanthiIsaka, B.L.; Silva, V.R.S.D. Hydraulic fracturing under high temperature and pressure conditions with micro CT applications: Geothermal energy from hot dry rocks. *Fuel* **2018**, *230*, 138–154. [CrossRef]
16. Xu, T.; Zhang, Y.; Yu, Z.; Hu, Z.; Guo, L. Laboratory study of hydraulic fracturing on hot dry rock. *Sci. Technol. Rev.* **2015**, *33*, 35–39.
17. Zhou, Z.; Jin, Y.; Zeng, Y.; Zhang, X.; Zhou, J.; Zhuang, L.; Xin, S. Investigation on fracture creation in hot dry rock geothermal formations of China during hydraulic fracturing. *Investig. Fract. Creat. Hot Dry Rock Geotherm. Form. China Dur. Hydraul. Fract.* **2020**, *153*, 301–313. [CrossRef]
18. Frash, L.P.; Gutierrez, M.; Hampton, J. True-triaxial apparatus for simulation of hydraulically fractured multi-borehole hot dry rock reservoirs. *Int. J. Rock Mech. Min. Sci.* **2014**, *70*, 496–506. [CrossRef]
19. Zhang, W.; Wang, C.; Guo, T.; He, J.; Zhang, L.; Che, S.; Qu, Z. Study on the cracking mechanism of hydraulic and supercritical CO2 fracturing in hot dry rock under thermal stress. *Energy* **2021**, *221*, 119886. [CrossRef]
20. Zhao, Y.; Wan, Z.; Feng, Z.; Dong, Y.; Yuan, Z.; Fang, Q. Triaxial compression system for rock testing under high temperature and high pressure. *Int. J. Rock Mech. Min. Sci.* **2012**, *52*, 132–138. [CrossRef]
21. Zhou, C.; Wan, Z.; Yuan, Z.; Gu, B. Experimental study on hydraulic fracturing of granite under thermal shock. *Geothermics* **2018**, *71*, 146–155. [CrossRef]